EVALUATING THE SMOKE HAZARD FROM FIRES IN LARGE SPACES

J.A. Milke
Associate Professor and Graduate Director, Department of Fire Protection Engineering
University of Maryland, College Park, MD 20742, USA

(Received 30 June 2000; Accepted 16 October 2000)

ABSTRACT

Current codes in many countries require that the smoke layer be maintained a particular distance above the highest walking surface in an atrium. The smoke exhaust capacity to accomplish the required performance can be extraordinary, especially in a tall atrium with the upper floors open to the atrium. The effect of exposure to smoke is a function of the magnitude of the smoke signature, e.g. concentration of gas species, visibility reduction and temperature, and the exposure duration. Generally, the first smoke layer property that reaches a critical level is a reduction in visibility. The visibility can be reduced below 1 m even though the temperature rise and generation of toxic gases are relatively modest. However, with a smoke exhaust rate of 200 kgs^{-1}, the hazard provided due to temperature rise and CO concentration in atria is modest for a wide range of fuels.

1. INTRODUCTION

The approach described in codes in many countries is based on maintaining the smoke layer interface a particular distance above the highest walking surface in an atrium (see Fig. 1). The associated smoke exhaust capacity required to provide a large clear height is substantial. Further, designers are also often concerned about the noteworthy make-up air requirements, especially given the U.S. requirement of a maximum velocity of 1.0 ms^{-1} for the make-up air. If the smoke exhaust capacity is substantial, then the area for the grilles for the make-up air will also be substantial.

However, because of the substantial clear height, air being entrained into the plume dilutes and decreases the hazard posed by the smoke. Consequently, the high-capacity exhaust fans may be removing smoke which poses relatively little threat to building occupants, indicating a design which is not cost-effective. An improved approach involves an analysis of the hazard posed by such smoke to identify a more reasonable smoke exhaust capacity.

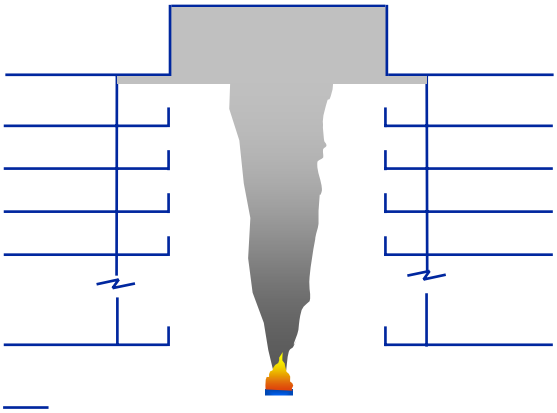

Fig. 1: Code-specified position of smoke layer in atrium

Appreciable attention is given in design guides to the parameters of an active smoke management system relative to achieving an equilibrium smoke layer position [1,2]. Less attention is devoted to assessing the development of hazard prior to activation of the system.

2. HAZARD LIMITS OF SMOKE

Smoke can adversely affect building occupants, fire brigade members, property (including the building structure and contents) and mission continuity. The effect of exposure to smoke is a function of the magnitude of the smoke signature, e.g. concentration of gas species, visibility reduction, temperature, radiant flux, etc., and the duration of the exposure.

People who are exposed to smoke may be harmed as a result of exposure to toxic gases, elevated temperature or radiant energy. The toxic effects of the gases in smoke are described in Purser [3] and Klote and Milke [4]. For short duration exposures (in the order of 1 to 2 mins), a carbon monoxide concentration of 0.1 to 0.8% may cause humans to become incapacitated while walking or being involved in a similar level of activity [3].

Exposure to radiant energy from a smoke layer of 2 to 5 kWm^{-2} for a short duration (5 to 10 seconds) is sufficient to inflict pain. Such a radiant exposure requires a smoke layer temperature of at least 160°C (considering the radiant flux emitted by a black body). People can typically tolerate being submerged in a smoke layer up to 100°C for approximately 10 minutes.

In addition, smoke may reduce visibility. A reduction of visibility may cause people evacuating to become disoriented or reduce their walking speed, thereby increasing the amount of time that they are exposed to the effects of smoke [5]. Klote and Milke [4] describe the relationship between visibility and movement speed [4]. In addition, a reduction of visibility may increase the susceptibility of building occupants to trip over obstructions or even fall over balcony railings [6]. Numerous individuals have proposed limits of optical density, ranging from 0.04 to 0.30 m^{-1} [7-13].

Building contents can be affected by exposure to corrosive gases, particulate matter, and elevated temperature of smoke. Contents may be damaged by temperatures and gas concentrations well below that needed to harm humans. Contents exposed to heated smoke may be melted, distorted or charred, depending on the temperature of the smoke and degree of exposure. Electronic equipment and data storage media are particularly sensitive to elevated temperature, being damaged at temperatures as low as 40°C for diskettes and 80°C for computer hardware [14]. Smoke may contain several corrosive components, either airborne or in some cases absorbed into solid particulates. Exposure to smoke containing only 0.01% of HCL or 0.1% of HF, can damage electronic equipment, especially if restoration activities are not initiated promptly after the incident.

Mission continuity may be threatened following a fire, as a building or portion thereof is closed for restoration. This results in loss of revenue for the building owner, temporary unemployment of workers in the building, and loss of service of the facility to the community, among other effects.

3. RECENT HISTORY OF U.S. REQUIREMENTS

A brief overview of the recent history of U.S. requirements for atrium smoke management is useful to appreciate the attitudes toward various calculation approaches. In the 1970's, the smoke exhaust capacity was required to be 4 to 6 air changes per hour. Because normal HVAC design often sought to provide 4 to 6 air changes per hour, it is suspected that the initial smoke exhaust requirement was based on using the HVAC fans, but in a different mode of operation. In the 1980's, it was recognized that the air change per hour requirement did not relate to limiting the level of hazard posed by smoke in a particular atrium. The initial version of NFPA 92B [1] identified a new design approach based on limiting hazard development in the atrium. This approach emphasized establishing a steady smoke layer position. The steady smoke layer position is the result of establishing equilibrium between the smoke exhaust rate and the smoke production rate. This concept has been in the literature since the 1960's and was originally adopted as the basis of designs for natural vents [15,16].

Many of the U.S. codes adopted this revised approach for smoke management in atria, requiring that the smoke layer be kept at a height of 1.8 to 3.0 m above the highest walking level, depending on the code. The requirements were based on preventing the smoke from descending to breathing level of a standing individual. This is a conservative strategy of providing protection from the hazard of smoke, independent of the qualities of the smoke.

Assessing the hazard from smoke is not currently discussed by any of the U.S. prescriptive codes, even though NFPA 92B [1] has included calculation methods for such an analysis since 1995. The new performance based chapter in the Life Safety Code [17] does refer to tenability calculations that would require a hazard assessment to be conducted as a prerequisite. Nonetheless, in some special cases, engineers have conducted a hazard assessment by considering the properties of the smoke layer and demonstrating the modest hazard associated with such smoke. These special analyses are usually motivated by engineers seeking relief from either the very large exhaust capacities or the associated intake air requirements required for tall atria.

This paper seeks to describe the engineering principles supporting these calculations. In addition, the paper explores the sensitivity of the results to various input parameters.

4. ESTIMATING THE EQUILIBRIUM SMOKE LAYER POSITION

The hazard posed by smoke is expressed in terms of the depth and properties of the smoke layer. An assessment of smoke hazard development can be conducted by applying engineering principles in the form of algebraic equations, small-scale physical models and computer-based zone and CFD models [18,19]. Only the algebraic equations are reviewed in this paper given the emphasis on reviewing the influence of selected parameters on the level of smoke hazard from fires in atria. Reviews of the small-scale physical models and computer-based models are available elsewhere [20,21].

The combustion products generated by building fires are principally dependent on the behavior of the fire. The proportion of gaseous, liquid and solid matter generated by the combustion process is dependent on the fuel, burning mode (flaming versus smoldering) and ventilation conditions. Air is entrained into the flaming region to support the combustion process. In

the region between the base and tip of the flames, only about 10% of the entrained air is consumed by the combustion process, with the remainder acting to dilute the combustion products [22]. Heat from the fire makes the combustion products and entrained air buoyant, causing them to rise in the form of a plume. Air is also entrained along the entire height of the smoke plume below a smoke layer. The entrained air has two effects:

- increases the mass flow in the plume to increase the quantity of "smoke" produced and
- dilutes the combustion products and decreases the temperature of the smoke to decrease the hazard of the smoke.

Considering the mechanics of smoke production within the flaming region and along the height of the plume, the tall ceiling height in some atria poses both as a challenge for successful smoke management and as a source of relief. The challenge is posed by the substantial production rate of smoke along a tall plume. However, smoke accumulating at the top of a tall space may be appreciably diluted to decrease the smoke hazard, but also to delay the response of ceiling mounted detectors or sprinklers.

4.1 Smoke Production Rate

Because smoke is predominantly composed of entrained air, the rate of smoke production can be estimated by the rate of air entrainment. There are several correlations available in the literature to estimate the rate of air entrainment [23]. One pair of correlations by Heskestad is included in NFPA 92B [1]. One of Heskestad's correlations is applicable as long as the average flame height is below the smoke layer, while the other is applicable to the case where flames reach or extend into the smoke layer. An estimate of the flame height is presented as equation (1) [1]:

$$z_f = 0.166\dot{Q}_c^{2/5} \qquad (1)$$

The convective portion of the heat release rate is that portion of the heat generated by the fire which is released from the flame plume convectively. The convective portion of the heat release rate is typically assumed to be approximately 70% of the total heat release rate, *i.e.* $\dot{Q}_c = 0.7\dot{Q}$ [1].

The correlation for entrainment of air into the plume, applicable as long as the clear height (height from the top of the fuel to the smoke layer interface) is greater than the average flame height, i.e. $z > z_f$, is provided as equation (2) [24]:

$$\dot{m} = 0.071\dot{Q}_c^{1/3} z^{5/3} + 0.0013\dot{Q}_c \qquad (2)$$

Equation (2) by Heskestad is of the same functional form as most other plume entrainment equations, differing by the coefficient of the $\dot{Q}_c^{1/3} z^{5/3}$ term and also the presence of the second term. (Generally for tall clear heights, the second term in equation (2) is much smaller than the first term.) Coefficients range from 0.066 to 0.124, with a mean of 0.086.

Alternatively, if flames are expected to reach the smoke layer ($z_f > z$), then the air entrainment is estimated by:

$$\dot{m} = 0.032\dot{Q}_c^{3/5} z \qquad (3)$$

As indicated in equations (2) and (3), the amount of air entrained is proportional to $z^{5/3}$ or z. The smoke production rate is presented as a function of heat release rate and clear height in Fig. 2, as determined by equations (2) and (3) over the appropriate range of clear heights. For fire sizes ranging from 1.0 to 10 MW, the flame heights range from 2.3 to 5.7 m (as estimated from equation (1)).

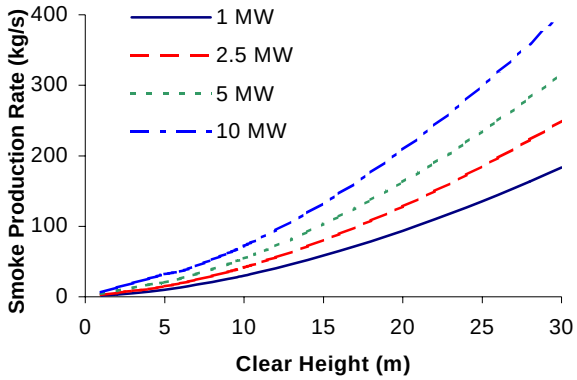

Fig. 2: Smoke production rate

In many atria, the ceiling height is greater than the flame height, with equation (2) being applicable (as long as the heat release rate of the fire is limited to a reasonable value). Where equation (2) applies, the smoke production rate is much more sensitive to the clear height than the fire size. This is fortunate in design applications, as the clear height is generally easier to determine than predicting the fire size.

In order to satisfy the common building code requirements, the mass flow of the exhaust is commonly equated to the mass entrainment rate determined from equation (2). If a large clear height is required, the mass exhaust rate is likely to be appreciable. Hansell and Morgan [25] suggest that a mass exhaust rate exceeding 200 kgs^{-1} may not be economically practical. If this is the case, then the maximum clear height provided by an exhaust rate of 200 kgs^{-1} ranges from 20 to 30 m, depending on the fire size. If the tallest walkway is at least 20 m above

the top of the fuel, then people or objects will be submerged in the smoke. In such cases, assessing the acceptability of a design with a maximum mass exhaust rate of 200 kgs^{-1} requires an estimation of the properties of the smoke layer and an assessment of the commensurate hazard.

5. PROPERTIES OF SMOKE LAYER

A zone model approach can be used to estimate the smoke layer properties from a pre-flashover fire. A zone model assumes that properties of a smoke layer are uniform throughout the volume of the smoke layer. As such, properties are independent of elevation within the layer or horizontal distance from the plume. As will be evident in each of the equations included in this section, the smoke layer properties are independent of the horizontal area occupied by the smoke layer. This is a result of the steady state condition being considered.

The following properties are of interest in evaluating the hazard posed by smoke, e.g. for tenability analyses or damage assessments.

- temperature
- gas species concentration
- light obscuration/visibility

5.1 Temperature

The temperature of the smoke layer can be determined based an energy balance for the smoke layer [18]:

$$\dot{Q}_c = (1-\chi_l)\dot{m}_e c_p \Delta T \qquad (4)$$

For the equilibrium condition assumed in this paper, the mass rate of exhaust is equal to the mass rate of smoke supply to the smoke layer, i.e. $\dot{m}_e = \dot{m}$.

Estimates for χ_l vary appreciably. Most of the design guides suggest that the smoke layer may be assumed to be adiabatic, *i.e.* $\chi_l = 0$, given the uncertainty in χ_l in order to be conservative [1,2]. Walton suggested values for χ_l between 0.6-0.9 for relatively small spaces of near cubic shape [26]. In part, this assumption is suggested due to the lack of information to suggest otherwise. As a result of the adiabatic assumption, predicted smoke layer temperatures will be greater than would actually occur.

In many atria with tall ceiling heights, the temperature rise anticipated for the smoke layer is relatively modest such that convection and radiation heat transfer to an enclosure may be minimal. In such cases, the adiabatic analysis provides a reasonable estimate of the temperature rise. However, in short ceiling spaces (under approximately 10 m), the temperature may be significantly overestimated by applying the adiabatic assumption.

An estimate of the heat loss factor can be obtained through an analysis of data obtained in the recent hangar tests conducted by the US Navy [27]. While this data is for a transient case because no venting was provided in the tests, the heat loss factor can be considered independent of whether transient or steady-state conditions was present. The time-dependent temperature rise is given in equation (5) [28]:

$$\Delta T = T_o\left[exp\left(\frac{(1-\chi_l)\dot{Q}t}{\rho_o c_p T_o V_u}\right)-1\right] \qquad (5)$$

Fig. 3 depicts the conditions associated with test #2. The overall ceiling height is 14.9 m, with a 24.4 x 18.3 m area of the ceiling enclosed by 3.7 m deep draft curtains. The fire source consisted of a 0.6 m square pan of JP-5. Full pan involvement was observed approximately 10 s after ignition. After full pan involvement was achieved, the fire had a near-steady heat release rate of 500 kW (determined based on a measurement of mass loss). The temperature of the smoke layer was measured by two thermocouples located 0.31 m from the ceiling, with one being 3.1 m and the other 6.3 m horizontally from the plume centerline.

The temperature of the smoke layer was estimated using equation (5). A trial and error approach was applied, considering three values of the heat loss fraction, 0, 0.3 and 0.7 in the three iterations. The temperature rise of the smoke layer was estimated at the point where visual observations indicated that the smoke had just filled the curtained area. The data and results of the analysis are presented in Fig. 4. As indicated in the figure, a heat loss fraction of 0.7 provides the best estimate of the temperature of the smoke layer. This heat loss fraction is comparable to that suggested for low height spaces.

Rearranging equation (4):

$$\frac{\dot{m}_e}{\dot{Q}} = \left(\frac{\lambda}{1-\chi_l}\right)\frac{1}{c_p \Delta T} \qquad (6)$$

Applying a heat loss fraction of 0.7, the temperature of the smoke layer is presented in Fig. 5 for a range of mass exhaust rates, including 200 kgs^{-1}. For a mass exhaust rate of 200 kgs^{-1}, the estimated temperature rise ranges from 9 to 35 °C for fire sizes between 1 and 10 MW. Even for a temperature rise of 35°C, the resulting smoke layer temperature is on the order of 55°C, which most individuals can tolerate for at least 10 mins [3]. As such, based on the anticipated temperature of the smoke layer, providing additional

exhaust capacity above 200 kgs^{-1} would have minimal benefit for design fire sizes up to 10 MW.

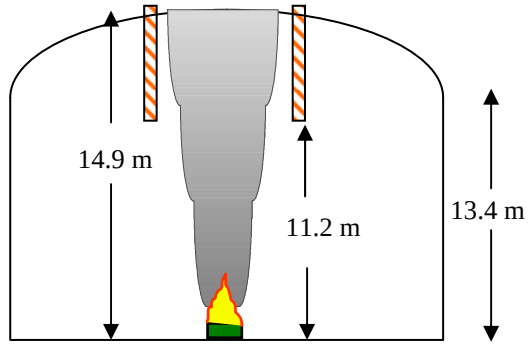

Elevation view

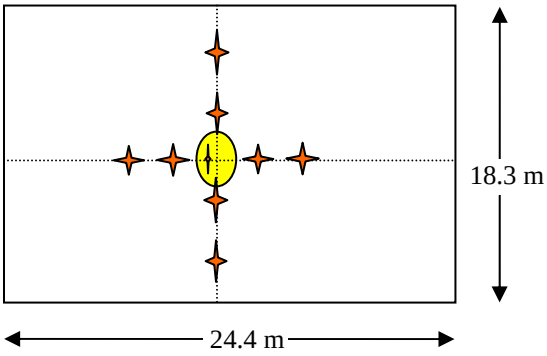

Plan view

Fig. 3: Schematic diagram, US Navy hangar test #2

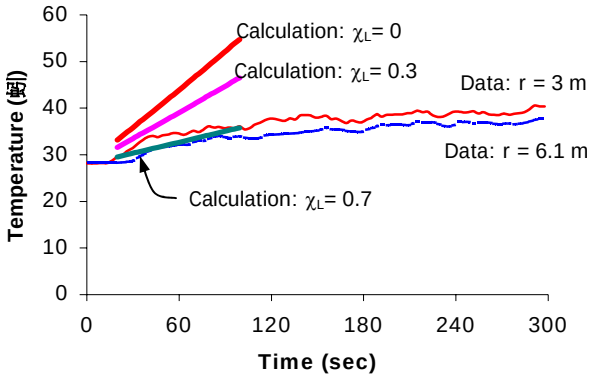

Fig. 4: Temperature of smoke layer – US Navy hangar test #2

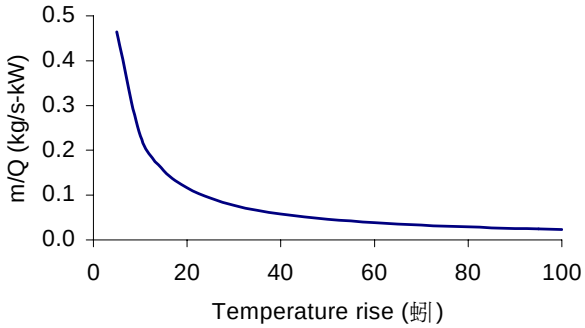

Fig. 5: Temperature rise vs. mass exhaust rate and heat release rate

5.2 Gas Species Concentration

The steady state expression for the concentration of gas species contained in the smoke layer can be developed considering the mass fraction of gas specie, i, in the smoke layer. No losses of the gas specie, either due to absorption by the enclosure or chemical reactions, is assumed [18].

The mass fraction of specie "i" in the smoke layer is defined as:

$$Y_i = \frac{\dot{m}_i}{\dot{m}_e} \tag{7}$$

where: $$\dot{m}_i = f_i \dot{m}_f = \frac{f_i \dot{Q}}{\chi_a \Delta H_c} \tag{8}$$

Substituting equation (8) into equation (7):

$$Y_i = \frac{f_i \dot{Q}}{\dot{m}_e \chi_a \Delta H_c} \tag{9}$$

Rearranging the terms in equation (9):

$$\frac{\dot{m}_e}{\dot{Q}} = \frac{f_i}{\chi_a \Delta H_c} \frac{1}{Y_i} \tag{10}$$

A volumetric proportion of the gas concentration, C_i, (in terms of ppm) is given as:

$$C_i = \frac{MW_{air}}{MW_i} Y_i \times 10^6 \tag{11}$$

Replacing Y_i with C_i provides the following equation:

$$\frac{\dot{m}_e}{\dot{Q}} = \frac{f_i}{\chi_a \Delta H_c} \frac{10^6}{C_i} \frac{MW_{air}}{MW_i} \tag{12}$$

The left hand side of equation (12) is a ratio of the mechanical exhaust with the heat release rate of the fire.

The CO fuel parameter, $f_i / \chi_a \Delta H_c$, is a fuel dependent parameter. The CO fuel parameter is provided in Table 1 for selected fuels that span a wide range of values of the parameter [29]. The yield fraction, f_i, is dependent on the burning mode and oxygen concentration. Values of the CO fuel parameter noted in Table 1 are based on data for the yield fraction from well-ventilated, flaming combustion of relatively small samples [29]. While most of the fires of interest in atria involve flaming combustion and are likely to be well-ventilated, the yields for actual fuel packages may be somewhat different than those reported for the small samples. For example, the CO_2 yield for an actual fuel package is likely to be slightly less than that reported for small samples and that for CO slightly greater. Fires in small, connected spaces may become under-ventilated. The yield fraction can vary by orders of magnitude for different ventilation conditions [29]. Also, the yield fractions noted by Tewarson are relevant only to cases where sprinklers are not operating [30].

The ratio of the mass exhaust and heat release rates needed to limit the CO concentration in the smoke layer for a range of CO fuel parameters is presented in Fig. 6. For the proposed maximum mass exhaust rate of 200 kgs^{-1}, the resulting CO concentration for a fire involving a particular fuel is a function of the heat release rate only:

$$C_i = 5000 \frac{f_i}{\chi_a \Delta H_c} \frac{MW_{air}}{MW_i} \dot{Q} \qquad (13)$$

Fig. 7 presents the results of applying equation (13) for heat release rates up to 10 MW. Considering that the CO fuel parameter is 2.5 x 10^{-6} $kgkJ^{-1}$ or less for all of the fuels noted in Table 1 except polyvinylchloride, the maximum CO concentration expected for the range of fire sizes noted in the figure is approximately 100 ppm. This concentration of CO would be expected to have little impact on people exposed for short durations.

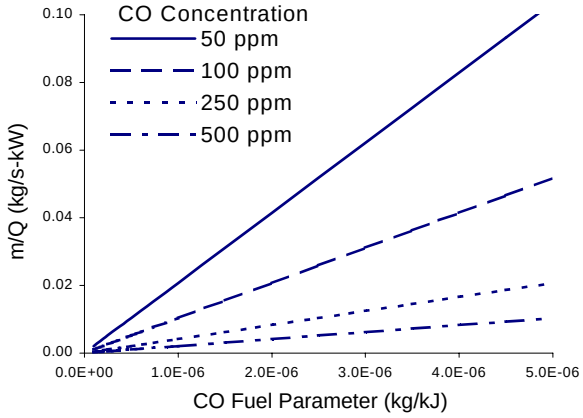

Fig. 6: CO concentration vs. mass exhaust rate and heat release rate

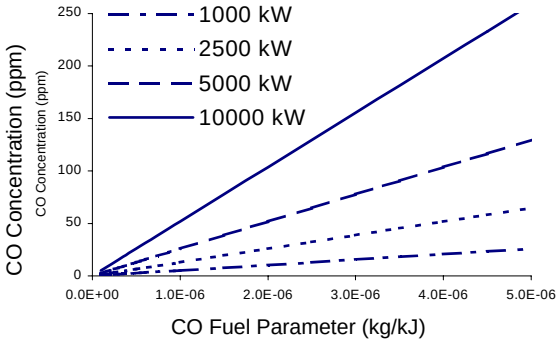

Fig. 7: CO concentration for a mass exhaust rate of 200 kgs^{-1}

Table 1: CO and visibility fuel parameters for selected fuels

Fuel	f_{CO} (kg CO/kg fuel)	D_m (m^2/g)	$\chi_a \Delta H_c$ (kJ/g)	$f_{CO}/\chi_a \Delta H_c$ (kg/kJ)x10^{-6}	$D_m/\chi_a \Delta H_c$ (m^2/kJ)x10^{-3}
Ethane	0.001	0.303	45.7	0.0219	6.63
Propane	0.005	0.112	43.7	0.114	2.57
Heptane	0.010	0.297	41.2	0.243	7.21
Styrene	0.065	0.899	27.8	2.34	3.23
Red oak	0.004	0.0576	12.4	0.323	4.64
Douglas fir	0.004	0.0636	13.0	0.308	4.89
Pine	0.005	0.0535	12.4	0.403	4.31
Polymethylmethacrylate	0.010	0.157	24.2	0.413	6.47
Polyethylene	0.024	0.382	38.4	0.625	9.95
Polypropylene	0.024	0.384	38.6	0.622	9.95
Polystyrene	0.060	0.806	27.0	2.22	29.9
Polystyrene foam	0.058-0.065	0.734-0.966	24.6-25.9	2.32-2.54	29.9-37.3
Nylon	0.038	0.382	27.1	1.40	14.1
Polyvinylchloride	0.063	0.709	5.7	11.2	124
Polyurethane foam	0.010-0.042	0.561-0.748	16.4-19.0	0.562-2.56	31.5-45.6

5.3 Optical Density

The optical density of the smoke layer can be determined considering that all of the particulates generated by the fire are transported to the layer via the plume and accumulate in the layer. Any plating out on enclosure surfaces and changes of optical density due to smoke aging is neglected [18]. The optical density can be related to the mass optical density, mass loss rate of fuel and volumetric exhaust capacity:

$$D = \frac{D_m \dot{m}_f}{\dot{V}_e} \tag{14}$$

Substituting for the mass burning rate, as done in equation (7), replacing the volumetric exhaust rate with the mass exhaust rate and rearranging:

$$\frac{\dot{m}_e}{\dot{Q}} = \rho_o \frac{D_m}{\chi_a \Delta H_c} \frac{1}{D} \tag{15}$$

The visibility of a lighted exit sign can be related to the optical density [4]:

$$S = \frac{0.43K}{D} \tag{16}$$

Using equation (16) to replace the optical density in equation (15) with K = 6 for back-lit exit signs results in:

$$\frac{\dot{m}_e}{\dot{Q}} = \frac{\rho_o}{0.43K} \frac{D_m}{\chi_a \Delta H_c} S \tag{17}$$

The term $D_m / \chi_a \Delta H_c$ is referred to as the visibility fuel parameter. As with the yield fraction in the calculation of the gas species concentration, the mass optical density is dependent on the fuel, burning mode, ventilation conditions and operation of sprinklers. The mass optical density can vary by orders of magnitude for different ventilation conditions [29]. The visibility fuel parameter is provided in Table 1 for selected fuels that span a wide range of values of the parameter [29,31].

Results of applying equation (17) are presented in Fig. 8. Solving equation (17) for the visibility distance for a mass exhaust rate of 200 kgs^{-1}, yields:

$$S = \frac{200}{\dot{Q}} \left[\frac{\rho_o}{0.43K} \frac{D_m}{\chi_a \Delta H_c} \right]^{-1} \tag{18}$$

The relationship of visibility to heat release rate and the visibility fuel parameter for a mass exhaust rate of 200 kgs^{-1} is presented in Fig. 9. Considering that the visibility fuel parameter is 0.030 m^{2}kJ^{-1} for most of the fuels noted in Table 1, the visibility through a smoke layer with only 200 kgs^{-1} of exhaust will be reduced significantly, depending on the fuel and combustion conditions.

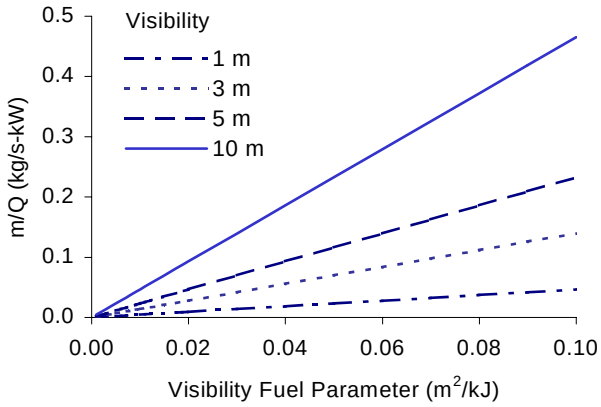

Fig. 8: Visibility through smoke vs. mass exhaust rate and heat release rate

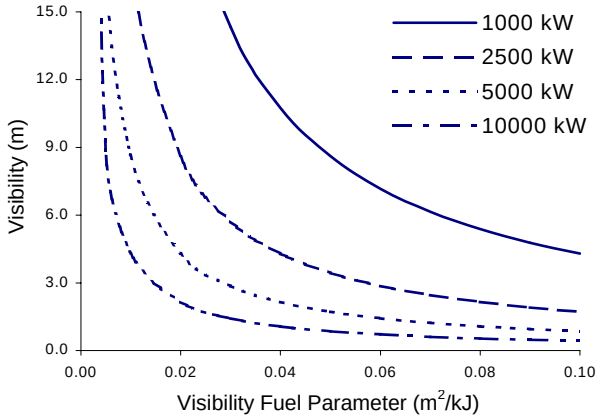

Fig. 9: Visibility through smoke for a mass exhaust rate of 200 kgs^{-1}

6. COMPARISON OF HAZARD POSED BY SMOKE LAYER PROPERTIES

The magnitude of the three smoke layer properties discussed in this paper, i.e. temperature, gas species concentration and optical density can be compared to assess which property is likely to dictate the acceptability of a particular design. Temperature rise can be related to gas species concentration by equating equations (6) and (12):

$$\frac{C_i}{\Delta T} = \frac{f_i}{\chi_a \Delta H_c} \frac{10^6 (1 - \chi_l) c_p}{\lambda} \frac{MW_{air}}{MW_i} \tag{19}$$

This relationship is applicable only given the range of conditions noted previously, i.e. flaming, well-ventilated fires. Equation (19) can be reformulated to provide a relationship between CO concentration and temperature rise, with the following substitutions:

χ_l:	0.7	λ:	0.7
c_p:	1.005 kJkg^{-1}°C^{-1}	MW_{air}:	29 kg
MW_{CO}:	28 kg		

$$C_{CO} = 0.45x10^6 \frac{f_i}{\chi_a \Delta H_c} \Delta T \qquad (20)$$

Fig. 10 depicts the linear relationship between temperature rise and CO concentration. For the range of CO fuel parameters considered, the CO concentration is modest if the temperature rise is modest. As such, for situations where ordinary sprinklers (operating temperature of 74 °C) are not expected to activate, i.e. for a temperature rise of 50°C or less, the hazard due to CO concentration in the smoke layer is minimal.

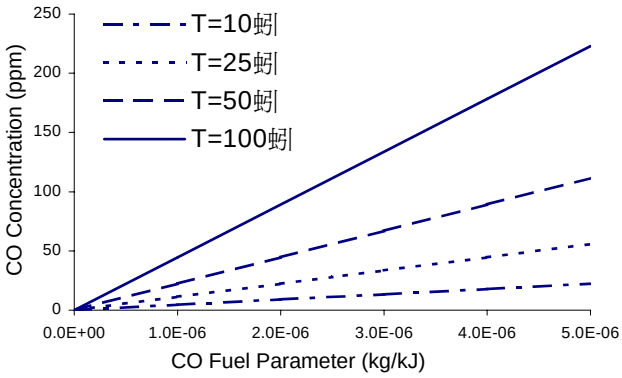

Fig. 10: Temperature rise vs. CO concentration in smoke layer

Similarly, a relationship between visibility and temperature rise is obtained by equating equations (6) and (17) and one for visibility and CO concentration by equating equations (12) and (17).

$$S = \frac{0.43K}{\rho_o} \frac{D_m}{\chi_a \Delta H_c} \left(\frac{\lambda}{1-\chi_l} \right) \frac{1}{c_p \Delta T} = 5.0 \frac{D_m}{\chi_a \Delta H_c} \frac{1}{\Delta T} \qquad (21)$$

$$S = \frac{f_i}{D_m} \frac{0.43x10^6 K}{\rho_o} \frac{MW_{air}}{MW_{CO}} \frac{1}{C_i} = 0.37x10^6 \frac{f_i}{D_m} \frac{1}{C_{CO}} \qquad (22)$$

The results of applying equations (21) and (22) are presented in Figs. 11 and 12. In both cases, the visibility reduction is substantial, even though the hazard due to temperature or CO concentration is relatively minor from the range of fuels and fire sizes considered.

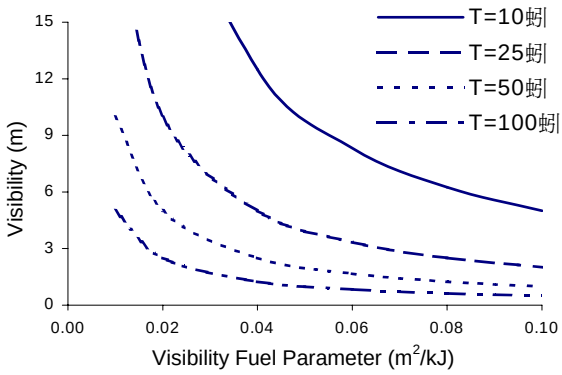

Fig. 11: Visibility vs. temperature rise in smoke layer

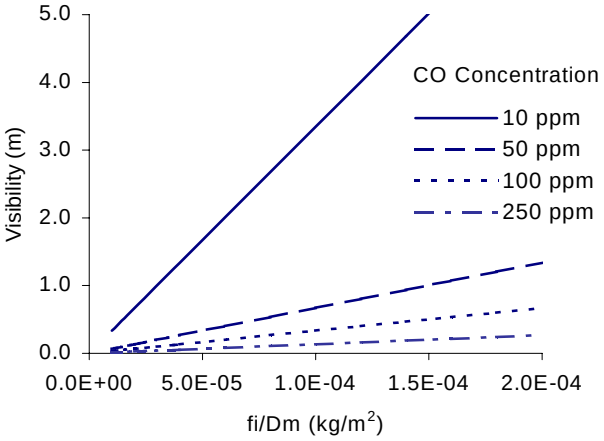

Fig. 12: Visibility vs. CO concentration in smoke layer

7. SUMMARY

Estimates of the smoke layer properties can be obtained using algebraic equations. An analysis of steady state conditions can be applied to ascertain the level of hazard posed by the smoke. The influence of key parameters on the smoke layer properties was provided. Generally, the benefit of providing smoke exhaust in excess of 200 kgs^{-1} appears to be relatively modest. For flaming, well-ventilated fires, the first smoke layer property which reaches a critical level is a reduction in visibility. The visibility can be reduced to 1 m or less even though the temperature rise and CO concentration are relatively modest.

NOMENCLATURE

C_i concentration of gas specie "i" (ppm)
C_{CO} concentration of CO (ppm)

c_p specific heat of ambient air (1.005 $kJkg^{-1}K^{-1}$)
D optical density (m^{-1}) *
D_m mass optical density (m^2kg^{-1})
f_i yield fraction of specie "i" (kg of specie "i" per kg of fuel consumed)
ΔH_c heat of combustion ($kJkg^{-1}$) #
K constant, depending on target being viewed, e.g. = 6 for lighted signs
MW_{air} molecular weight of air (kg)
MW_{CO} molecular weight of CO (kg)
MW_i molecular weight of specie "i" (kg)
$\dot{m}$ mass rate of air entrainment (kgs^{-1})
$\dot{m}_e$ mass exhaust rate (kgs^{-1})
$\dot{m}_f$ mass loss rate of fuel (kgs^{-1})
$\dot{m}_i$ mass generation of specie "i" (kgs^{-1})
$\dot{Q}$ heat release rate of fire (kW)
$\dot{Q}_c$ convective portion of heat release rate of fire (kW)
S visibility distance to exit sign (m)
ΔT temperature rise of smoke layer (°C)
T_o temperature of ambient air (293 K)
V_u volume of upper smoke layer (m^3)
$\dot{V}_e$ volumetric exhaust rate (m^3s^{-1})
Y_i mass fraction of gas specie "i" (kg of specie "i" per kg of smoke)
z height above top of fuel to smoke layer interface (m)
z_f average flame height (m)
χ_a combustion efficiency
χ_l heat loss fraction from smoke to enclosure
λ ratio of heat released convectively to the total heat release rate
ρ_o density of ambient air (1.2 kgm^{-3})

REFERENCES

1. NFPA 92B, Guide for smoke management systems in malls, atria, and large areas, NFPA (1995).
2. CIBSE, Relationships for smoke control calculations, TM 19, Chartered Institution of Building Services Engineers, London (1999).
3. D.A. Purser, Toxicity assessment of combustion products, In: P.J. DiNenno (editor), SFPE Handbook of Fire Protection Engineering, 2nd edition, NFPA (1995).
4. J.H. Klote and J.A. Milke, Design of smoke management systems, American Society of Heating, Refrigerating and Air-Conditioning Engineers (1992).
5. T. Jin, "Irritating effects of fire smoke on visibility", Fire Science and Technology, Vol. 5, No. 1, pp. 79-90 (1985).
6. J. Morehart, "Sprinklers in the NIH Atrium: How did they react during the fire last May?", Fire J., Vol. 83, No. 1, pp. 56-57 (1989).
7. G.T. Tamura, Smoke movement and control in high-rise buildings, NFPA (1994).
8. T. Jin, "Visibility through fire smoke", J. of Fire and Flammability, Vol. 9, pp. 135-155 (1978).
9. K. Kawagoe and H. Saito, "Measures to deal with smoke problems caused by fire", J. of Japan Society for Safety Engineering, Vol. 6, No. 7, pp. 108-114 (1967).
10. T. Wakamatsu, Calculation of smoke movement in buildings, Building Research Institute Research Paper No. 34, (1968).
11. Los Angeles Fire Department, Operation school burning, No. 2, NFPA (1961).
12. D.J. Rasbash, "Smoke and toxic products produced at fires", Transactions and Journal of Plastics Institute, pp. 55-61 (1967).
13. H.L. Malhotra, Movement of smoke on escape routes, instrumentation and effect of smoke on visibility, FR Notes 651, 652, 653, Borehamwood, UK (1967).
14. NFPA 75, Standard for the protection of electronic computer/data processing equipment, NFPA (1999).
15. P.H. Thomas and P.L. Hinkley, Design of roof-venting systems for single-storey buildings, Fire Research Technical Paper No. 10, Fire Research Station (1964).
16. NFPA 204, Guide for smoke and heat venting, NFPA (1998).
17. NFPA 101, Life Safety Code, NFPA (2000).
18. J.A. Milke and F.W. Mowrer, A design algorithm for smoke management systems in atria and covered malls, Report FP 93-04, Report to American Society of Heating, Refrigerating and Air-Conditioning Engineers, University of Maryland (1993).
19. J.A. Milke and J.H. Klote, Smoke management in large spaces in buildings, Building Control Commission of Victoria and The Broken Hill Proprietary Company Limited, Melbourne, Australia (1998).
20. W.K. Chow, "Atrium smoke filling process in shopping malls in Hong Kong", J. of Fire Protection Engineering, Vol. 9, No. 4, pp. 18-30 (1999).

* The extinction coefficient,α, is equal to 2.303D. Replacing D with α in equation (17), the visibility is equal to the ratio of K/α.

In some references, the product of $\chi_a\Delta H_c$ is referred to as the effective or chemical heat of combustion.

21. J.A. Milke, “Smoke management system design aides using models”, Fire Protection Engineering, Vol. 22, No. 7, pp. 17-18 (2000).

22. M.A. Delichatsios, Air entrainment into buoyant jet flames and pool fires, In: P.J. DiNenno (editor), SFPE Handbook of Fire Protection Engineering, 2nd edition, NFPA (1995).

23. C.L. Beyler, “Fire plumes and ceiling jets”, Fire Safety J., Vol. 11, No. 1 & 2, pp. 53-76 (1986).

24. G. Heskestad, Engineering relations for fire plumes, SFPE TR 82-8, SFPE (1982).

25. G.O. Hansell and H.P. Morgan, Design approaches for smoke control in atrium buildings, Building Research Establishment (1994).

26. W.D. Walton, ASET-B: A room fire program for personal computers, NBSIR 85-3144, National Bureau of Standards (1985).

27. J.E. Gott, D.L. Lowe, K. A. Notarianni and W.D. Davis, Analysis of high bay hangar facilities for fire detector sensitivity and placement, NIST TN 1423, National Institute of Standards and Technology (1997).

28. F.W. Mowrer, “Enclosure smoke filling revisited”, Fire Safety J., Vol. 33, pp. 93-114 (1999).

29. A. Tewarson, Generation of heat and chemical compounds in fires, In: P.J. DiNenno (editor), SFPE Handbook of Fire Protection Engineering, 2nd edition, NFPA (1995).

30. G.D. Lougheed, Probability of occurrence and expected size of shielded fires in sprinklered building, Phase 2, Full-scale fire tests, National Research Council of Canada, Ottawa (1997).

31. G. Mulholland, Generation of heat and chemical compounds in fires, In: P.J. DiNenno (editor), SFPE Handbook of Fire Protection Engineering, 2nd edition, NFPA (1995).